

**NAVAL POSTGRADUATE SCHOOL  
Monterey, California**



**THESIS**

**RAIL EROSION AND PROJECTILE DIAGNOSTICS FOR  
AN ELECTRO-MAGNETIC GUN**

by

William Etheridge Culpeper

June 2002

Thesis Advisor: William B. Maier II  
Co-Advisor: Richard Harkins

**Approved for public release; distribution is unlimited.**

THIS PAGE INTENTIONALLY LEFT BLANK

**REPORT DOCUMENTATION PAGE**

 Form Approved OMB No.  
 0704-0188

Public reporting burden for this collection of information is estimated to average 1 hour per response, including the time for reviewing instruction, searching existing data sources, gathering and maintaining the data needed, and completing and reviewing the collection of information. Send comments regarding this burden estimate or any other aspect of this collection of information, including suggestions for reducing this burden, to Washington headquarters Services, Directorate for Information Operations and Reports, 1215 Jefferson Davis Highway, Suite 1204, Arlington, VA 22202-4302, and to the Office of Management and Budget, Paperwork Reduction Project (0704-0188) Washington DC 20503.

1. AGENCY USE ONLY (Leave blank)	2. REPORT DATE	3. REPORT TYPE AND DATES COVERED
	June 2002	Master's Thesis
4. TITLE AND SUBTITLE Rail Erosion and Projectile Diagnostics for an Electro-Magnetic Gun		5. FUNDING NUMBERS
6. AUTHOR (S) Name		
7. PERFORMING ORGANIZATION NAME(S) AND ADDRESS(ES) Naval Postgraduate School Monterey, CA 93943-5000		8. PERFORMING ORGANIZATION REPORT NUMBER
9. SPONSORING / MONITORING AGENCY NAME(S) AND ADDRESS(ES)		10. SPONSORING/MONITORING AGENCY REPORT NUMBER
11. SUPPLEMENTARY NOTES The views expressed in this thesis are those of the author and do not reflect the official policy or position of the U.S. Department of Defense or the U.S. Government.		
12a. DISTRIBUTION / AVAILABILITY STATEMENT distribution statement		12b. DISTRIBUTION CODE
13. ABSTRACT (maximum 200 words)  Rail guns will not be introduced to the Navy until there is a means of limiting rail erosion. Erosion occurs when a sliding contact loses electrical contact with the rails. Research for this thesis was centered on combating the rail erosion problem and developing a way to record the voltage drop across the rails of the Naval Post Graduate School's 4-inch Electro-Magnetic Gun. A laser was also added to the rail gun so that the projectile's velocity could be recorded as it exits the gun's barrel. Silver paste was used to coat the grooved rails, thereby establishing a strong electrical contact between the rails and projectile. Results indicate that silver paste limits erosion inflicted on both the rails and projectile, by increasing the electrical contact at the rail-projectile interface. Consistent measurements of the projectile's velocity were also obtained.		
14. SUBJECT TERMS Rail Gun, Railgun, Sliding Contact, Electrical Contact, Conductive Interface, Silver Paste, Rail Erosion, Projectile Diagnostics		15. NUMBER OF PAGES 65
17. SECURITY CLASSIFICATION OF REPORT Unclassified	18. SECURITY CLASSIFICATION OF THIS PAGE Unclassified	19. SECURITY CLASSIFICATION OF ABSTRACT Unclassified
		20. LIMITATION OF ABSTRACT UL

NSN 7540-01-280-5500

 Standard Form 298 (Rev. 2-89)  
 Prescribed by ANSI Std. Z39-18

THIS PAGE INTENTIONALLY LEFT BLANK

**Approved for public release; distribution is unlimited.**

**RAIL EROSION AND PROJECTILE DIAGNOSTICS FOR AN ELECTRO-MAGNETIC GUN**

William Etheridge Culpeper  
Ensign, United States Navy  
B.S., United States Naval Academy, 2001

Submitted in partial fulfillment of the  
requirements for the degree of

**MASTER OF SCIENCE IN APPLIED PHYSICS**

from the

**NAVAL POSTGRADUATE SCHOOL**  
**June 2002**

Author:

William Etheridge Culpeper

Approved by:

William B. Maier II, Thesis Advisor

Richard Harkins, Co-Advisor

William B. Maier II, Chairman  
Department of Physics

THIS PAGE INTENTIONALLY LEFT BLANK

## **ABSTRACT**

Rail guns will not be introduced to the Navy until there is a means of limiting rail erosion. Erosion occurs when a sliding contact loses electrical contact with the rails. Research for this thesis was centered on combating the rail erosion problem and developing a way to record the voltage drop across the rails of the Naval Post Graduate School's 4-inch Electro-Magnetic Gun. A laser was also added to the rail gun so that the projectile's velocity could be recorded as it exits the gun's barrel. Silver paste was used to coat the grooved rails, thereby establishing a strong electrical contact between the rails and projectile. Results indicate that silver paste limits erosion inflicted on both the rails and projectile, by increasing the electrical contact at the rail-projectile interface. Consistent measurements of the projectile's velocity were also obtained.

THIS PAGE INTENTIONALLY LEFT BLANK

## TABLE OF CONTENTS

I.	INTRODUCTION .....	1
A.	PURPOSE .....	1
B.	HISTORY .....	1
1.	Why a Rail Gun for the U.S. Navy? .....	2
2.	Possible Parameters .....	3
C.	BASIC RAIL GUN THEORY .....	4
D.	BARREL WEAR .....	6
E.	MOTIVATION FOR THESIS .....	8
II.	THE EXPERIMENTAL METHOD .....	9
A.	EQUIPMENT USED .....	9
B.	THE POWER SUPPLY .....	10
C.	ADDED INDUCTANCE .....	11
D.	CURRENT DENSITY .....	15
E.	PARTS .....	17
1.	Accelerator .....	17
a.	Determining the Velocity of the Captive Bolt .....	18
2.	Pusher Housing .....	21
3.	Pusher Assembly .....	22
F.	TRIGGER BOX AND DELAY GENERATOR .....	23
G.	CONTACT BOX .....	23
H.	INTERIOR AND EXTERIOR DIAGNOSTICS .....	24
1.	Variable Graphite Resistor .....	24
2.	Laser for Projectile Velocity Measurement ...	26
I.	THERMAL LOADING OF RAILS .....	28
III.	TEST RESULTS .....	31
A.	STATIC TESTS WITH CONTACT BOX .....	31
B.	PROJECTILE VELOCITY RESULTS .....	34
C.	RESULTS WITH THE VARIABLE RESISTOR .....	35
1.	Static Tests With Variable Resistor .....	35
2.	Dynamic Tests With Variable Resistor .....	37
D.	RAIL EROSION .....	39
IV.	CONCLUSION .....	43
V.	FUTURE WORK .....	45
LIST OF REFERENCES .....		47
INITIAL DISTRIBUTION LIST .....		49

THIS PAGE INTENTIONALLY LEFT BLANK

## LIST OF FIGURES

Figure 1. Illustration of the Lorentz Force .....	4
Figure 2. Generated Magnetic Field .....	6
Figure 3. Erosion on rails from a shot with power supply capacitors charged to 5.5 kV .....	7
Figure 4. Schematic of the old power supply .....	10
Figure 5. Schematic of new power supply, output to Oscilloscope is 0.003 ohms from the grounded side of the rails. ....	11
Figure 6. Waveform of a current pulse. $L = 2.5 \mu H$ , $C = 1660 \mu F$ , $R = 9 m\Omega$ , voltage across capacitors, $V_c$ , is 2.25 kV. ....	12
Figure 7. Current pulse without inductor. The ordinate scale is 2 V per major division. The abscissa scale is 200 $\mu s$ per major division.....	14
Figure 8. Current pulse with inductor. Vertical sensitivity is 2 V per division. Horizontal sensitivity is 500 $\mu s$ per division.....	15
Figure 9. Current pulse. Ordinate scale is 2 V per division. Abscissa scale is 500 $\mu s$ per division.	16
Figure 10. Drawing of the accelerator .....	18
Figure 11. Picture of Laser Setup .....	19
Figure 12. Waveform of bolt passing through lasers. Ordinate and abscissa scales are 2 V per division and 500 $\mu s$ respectively.....	21
Figure 13. Pusher housing and assembly dimensions .....	22
Figure 14. Circuit of contact box .....	24
Figure 15. Laser and Variable Resistor Position .....	25
Figure 16. Dimensions of laser setup .....	27
Figure 17. Observed voltage for firing with bare rails. The ordinate and abscissa scales are 2 V per division and 500 $\mu s$ per division respectively....	32
Figure 18. Waveform of contact with silver paste. The vertical scale is 2 V per division. The horizontal scale is 200 $\mu s$ per division.....	33
Figure 19. Waveform of Projectile Position. The ordinate scale is 1 V per division. The abscissa scale is 1.00 ms per major division.....	34
Figure 20. Voltage across empty rails. The ordinate and abscissa scales are 2 V per division and 500 $\mu s$ per division respectively.....	36

Figure 21. Voltage across rails for a static projectile in good electrical contact. The ordinate and abscissa scales are 2 V per division and 500 $\mu$ s per division respectively. ....	37
Figure 22. Voltage drop when projectile traveled through dry grooved rails. The ordinate and abscissa scales are 2 V per division and 500 $\mu$ s per division respectively. ....	38
Figure 23. Voltage drop when projectile traveled through rails coated with silver paste. The ordinate and abscissa scales are 2 V per division and 500 $\mu$ s per division respectively. ....	39
Figure 24. Wear on dry grooved rails .....	40
Figure 25. Rails coated with silver paste before firing	41
Figure 26. Projectile and rails coated with silver paste after shot .....	42

## LIST OF TABLES

Table 1. Guide for a Fleet Rail Gun .....	3
Table 2. Cartridge Velocities .....	20
Table 3. Parameters for calculating $\frac{W}{Ax}$ .....	29

THIS PAGE INTENTIONALLY LEFT BLANK

## **ACKNOWLEDGEMENTS**

Throughout my thesis research I have received significant assistance from George Jaksha and Sam Barone. They were always willing to help build a part or find something that I needed, usually on extremely short notice.

I owe a special thanks to the Physics Department's faculty for their help in different areas of my research. Thank you to my thesis advisor, Bill Maier, for introducing me to the rail gun program at the Naval Post Graduate School, and then guiding me through my research process. I have learned many valuable concepts and lessons from him over the past year. Thank you to Richard Harkins, my co-advisor, for helping me with the editing process.

Over the course of my thesis research I worked very closely with Donald Snyder, day in and day out. He helped me with every area of my work. He is a brilliant man who knows everything there is to know about rail guns. I owe him sincere thanks, for he made it possible for progress to be made on the rail gun and allowed my thesis research to be completed.

THIS PAGE INTENTIONALLY LEFT BLANK

## I. INTRODUCTION

### A. PURPOSE

The purpose of this thesis is to use a four-inch-long test bed to investigate materials and configurations to be used in the projectile-rail interface of a high-velocity rail gun. Specific milestones for this thesis are to develop a way to record a projectile's velocity and to devise a means of determining the voltage drop across the rails, so that electrical contact between rails and a projectile can be monitored.

### B. HISTORY

The military's use of rail guns and electromagnetic launchers has been considered for years with much research and testing, but so far neither the rail gun nor an electromagnetic launcher is an integral part of any military weapon. The serious question that must be answered is, why not? The rail gun cannot be integrated into the fleet until a few key problems have been researched further and solved. First, the erosion the rails experience during a projectile or armature acceleration must be reduced. The military has no use for a one shot weapon.

## **1. Why a Rail Gun for the U.S. Navy?**

The Navy needs a weapon that can provide a consistent long-range threat to any target from the sea. The 5-inch Dual Purpose Guns deployed on ships throughout the world today simply do not have enough power to pose a real threat to our adversaries. The muzzle velocity that these chemically propelled gun systems are capable of giving to projectiles is around 800 meters per second [5].

Rail guns are capable of launching a projectile having velocities up to 2.8 km/s, which gives a range of approximately 300 nmi [1,4], depending projectile design. An easy way to determine whether or not a weapon will produce a kill is by calculating the energy that will be put into the target area. There are large efforts in the field of Electro-Thermal-Chemical (ETC) launch to increase the muzzle energy of the 5-inch gun systems [1]. Efforts thus far by researchers dedicated to ETC launch have been able to reach muzzle energies of 20 MJ, considerably larger than the typical 11 MJ muzzle energies that 5-inch guns provide. The muzzle energy for the CNA 2001 Notional Rail Gun is defined as 63 MJ [4]. The velocity of the projectile on the target depends on projectile design but could be 1.5 km/s with 17 MJ of kinetic energy on target. Energy from any explosive warheads present in the projectile would be added to the 17 MJ value.

The range of the projectile is just as important as speed and energy on target. The 5-inch DP guns used today have a range of approximately 10 to 15 nmi, much smaller than the 300 nautical mile range that the rail gun will

have [1,4]. This increase in range will allow naval vessels to stand off 100 nmi from the shore and be able to drop high velocity rounds 200 nmi inland. Because 85 percent of the world's population is within this range of an ocean, the rail gun is potentially a very lethal weapon system [4,9].

## **2. Possible Parameters**

The table below offers values for some important rail gun parameters. The values only serve as a guideline for what the Navy might use in the future [4].

Table 1. Guide for a Fleet Rail Gun

<b>Flight Mass</b>	<b>15 kg</b>
<b>Launch Body</b>	<b>20 kg</b>
<b>Launch Velocity</b>	<b>2.5 km/s</b>
<b>Muzzle Energy</b>	<b>63 MJ</b>
<b>Launch Acceleration</b>	<b>30-45 Kgees</b>
<b>Breech Energy</b>	<b>150 MJ</b>
<b>Barrel Length</b>	<b>10 Meters</b>
<b>Rounds Per Minute</b>	<b>6-10 RPM</b>

The flight mass differs from the mass of the launch body because a thin aerodynamic sabot round is the nominal projectile.

### C. BASIC RAIL GUN THEORY

The theory behind a rail gun is quite simple. Large amounts of current are passed through the rails and a sliding contact. This generates a magnetic field, which interacts with the current through the projectile and produces a force on the projectile. This Lorentz Force can be estimated from the following equation:

$$\overline{dF} = I(\vec{dl} \times \vec{B}) \quad (1.1)$$

Where the term  $d\vec{l}$  is an element of length along the current path through the projectile, and  $\overline{dF}$  is an element of force acting on the projectile. The variable  $I$  is the current through the projectile and  $B$  is the generated magnetic field.

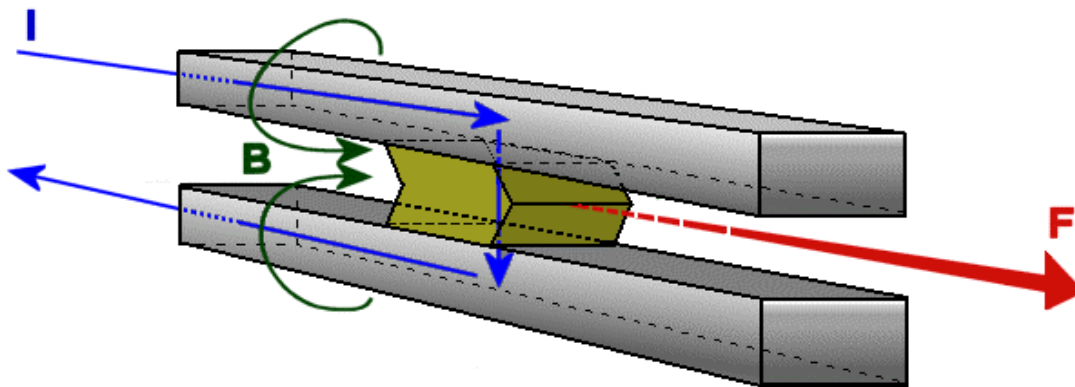


Figure 1. Illustration of the Lorentz Force

The Biot-Savart law for a semi-infinitely long straight wire is shown in the equation below:

$$\vec{B} = \frac{\mu_0 I}{4\pi r} \quad (1.2)$$

Equation 1.2 can be used to estimate the magnetic field between the rails. Here,  $\mu_0$  is the permeability of free space. The variable  $r$  is the radial distance from the center of the wire. In order to simplify the above equations, substitute Equation 1.2 into Equation 1.1 and integrate:

$$F = \frac{\mu_0 I^2}{4\pi} \int_R^{R+l} \left( \frac{1}{x} + \frac{1}{2R+l-x} \right) dx \quad (1.3)$$

Or,

$$F = \frac{\mu_0 I^2}{4\pi} \ln \left\{ \frac{(R+l)^2}{R^2} \right\} \quad (1.4)$$

Define  $L'$  as the inductance gradient with units of Henries per meter. The equation for the inductance gradient is given below.

$$L' = \frac{\mu_0}{2\pi} \ln \left\{ \frac{(R+l)^2}{R^2} \right\} \quad (1.5)$$

Although this treatment is approximate, the inductance gradient depends solely on the geometrical configuration of the rail gun.

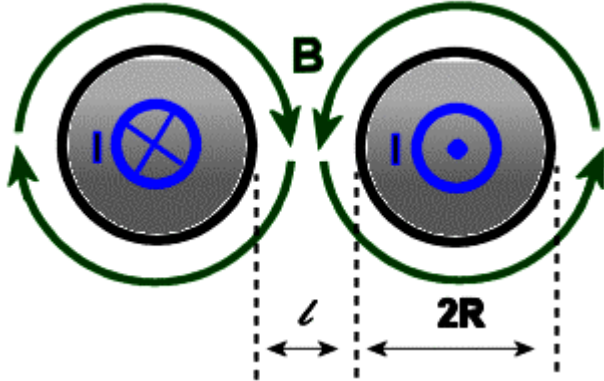


Figure 2. Generated Magnetic Field

Substitute Equation 1.5 into Equation 1.4:

$$F = \frac{1}{2} LI^2 \quad (1.6)$$

Equation 1.6 is the usual form for the force acting on a rail gun projectile [5].

#### D. BARREL WEAR

Analyzing the forces and stresses the projectile undergoes within the bore of the rail gun is vital. The strains that the projectile undergoes damage not only the projectile itself but also the bore. Firing damage to the bore must be minimized, especially if the weapon system is to be deployed on Navy Combatants where barrel replacement is not an easy task.

Barrel wear, or erosion, is frequently classified into three major areas: gouging, transition, deposition [1].

When gouging occurs inside the bore of a weapon system, pieces of the rails are removed by the passage of the projectile. Clearly, this limits the barrel's lifetime

severely. Transition refers to the damage inflicted upon both rails and projectiles when electrical contact cannot be maintained and arcing results. Erosion is a more gradual affect. With erosion, minuscule layers of the bore are wearing away during each fire. After a period of time, the entire barrel will have to be replaced. Deposition is when outer layers of the projectile are peeled off and spread along the bore.



Figure 3. Erosion on rails from a shot with power supply capacitors charged to 5.5 kv

Figure 3 shows what rail erosion looks like when approximately 60 kA of current runs through a projectile placed between 4 inch copper tungsten rails. The

projectile used was a piece of silver tungsten. The contact area was 0.25 inches long and 0.25 inches wide.

#### **E. MOTIVATION FOR THESIS**

So far, all of the rail gun research has not produced a weapon that is capable of being placed on a ship. The main goal of rail gun research is to work out the problems so that someday, this weapon system can be utilized at sea. The work done at NPS has focused on finding a method of minimizing the wear of the interface between the rails and projectiles when the rail gun is fired. To understand the complications created by erosion, better firing diagnostics must be developed.

## II. THE EXPERIMENTAL METHOD

### A. EQUIPMENT USED

The rail gun used for testing is the same test-bed Donald Gillich designed for his thesis [6]. Gillich used two 4-inch long rails to "investigate rail wear and rail-armature interface dynamics [6]." A major problem that arose when working with this rail gun was the issue of spacing. It is very difficult to align the rails to a point where the projectile experiences an equal amount of force from the rails along the entire 4 inches. To combat this problem, Mark Adamy replaced the phenolic spacer between the two rails used in Gillich's design with a more rigid 0.25-inch ceramic spacer [1]. This modification along with varying sizes of shims has improved rail alignment for the 4-inch gun.

Adamy used grooved 4-inch copper tungsten rails in the rail gun. The projectiles used for testing are 0.25 in wide and 0.25 in long, and are made out of silver tungsten. There is 0.0625 square inches of the projectile's surface in contact with each rail. Each projectile weighs about 3 g. Adamy further modified the rail gun Gillich constructed by adding three critical parts [1]. An accelerator was added so that the projectile would be moving, thereby overcoming static friction, when the capacitor bank is discharged. A pusher assembly and pusher housing were also added to transfer the energy from the accelerator to the projectile. The pusher is between the rails prior to

firing, and is in motion when the high power is applied to the rails.

### B. THE POWER SUPPLY

The power supply had to be reconfigured in order to measure the voltage across the rails. Measuring how well the armature or projectile is making electrical contact is accomplished by measuring the voltage difference across the two rails. Figure 4 shows both rails being held at high potential prior to firing. Since the previous design set both rails at high potential it was not convenient to measure the difference in voltage with our equipment.

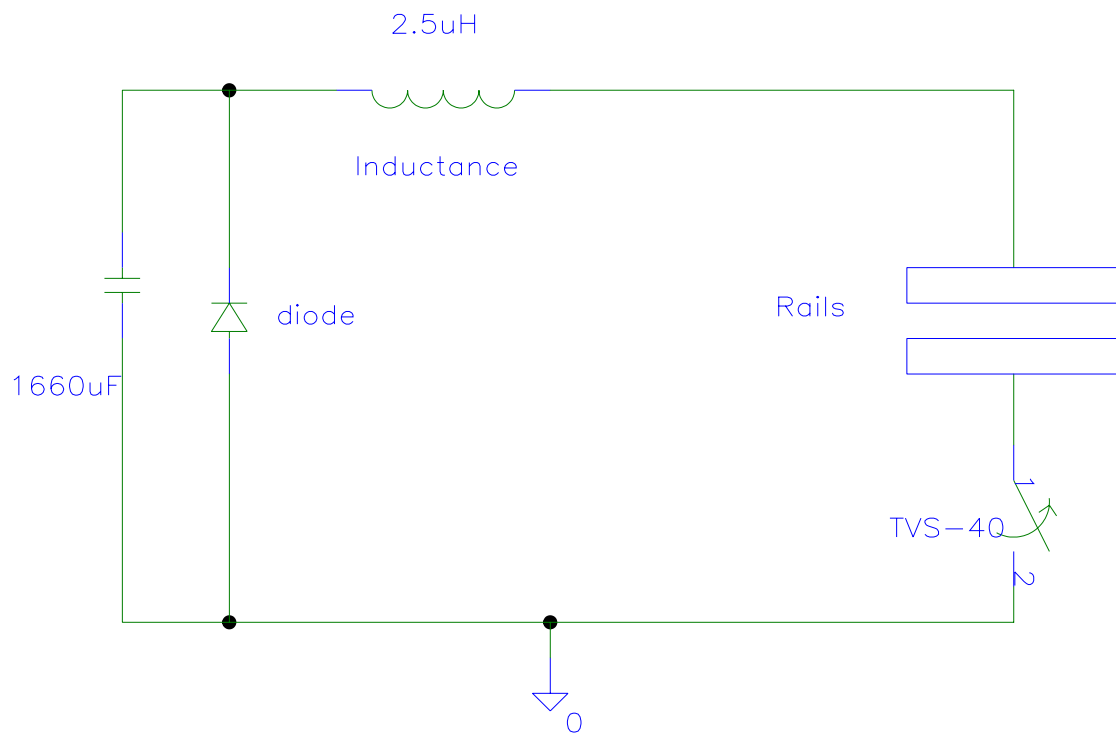


Figure 4. Schematic of the old power supply

The TVS-40 switch was moved in front of the rails, as seen in the Figure 5, to facilitate the voltage measurement across the rails.

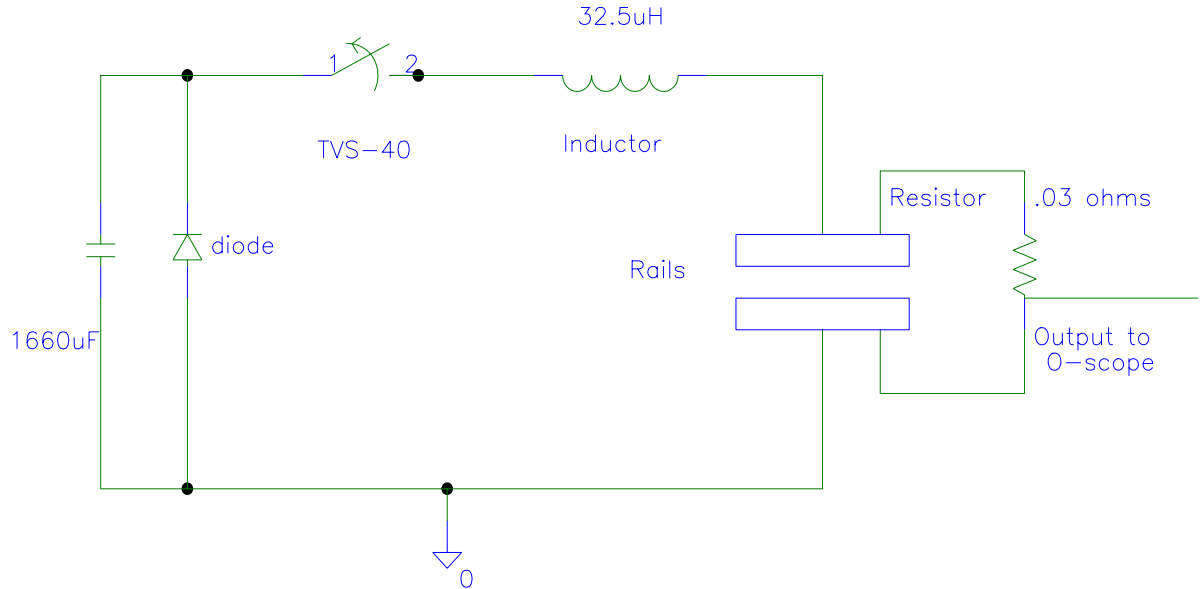


Figure 5. Schematic of new power supply, output to Oscilloscope is 0.003 ohms from the grounded side of the rails.

### C. ADDED INDUCTANCE

A theoretical plot of current versus time is shown in Figure 6. The rise is controlled by the circuit inductance and capacitance, and the decay by the circuit inductance and resistance [5].

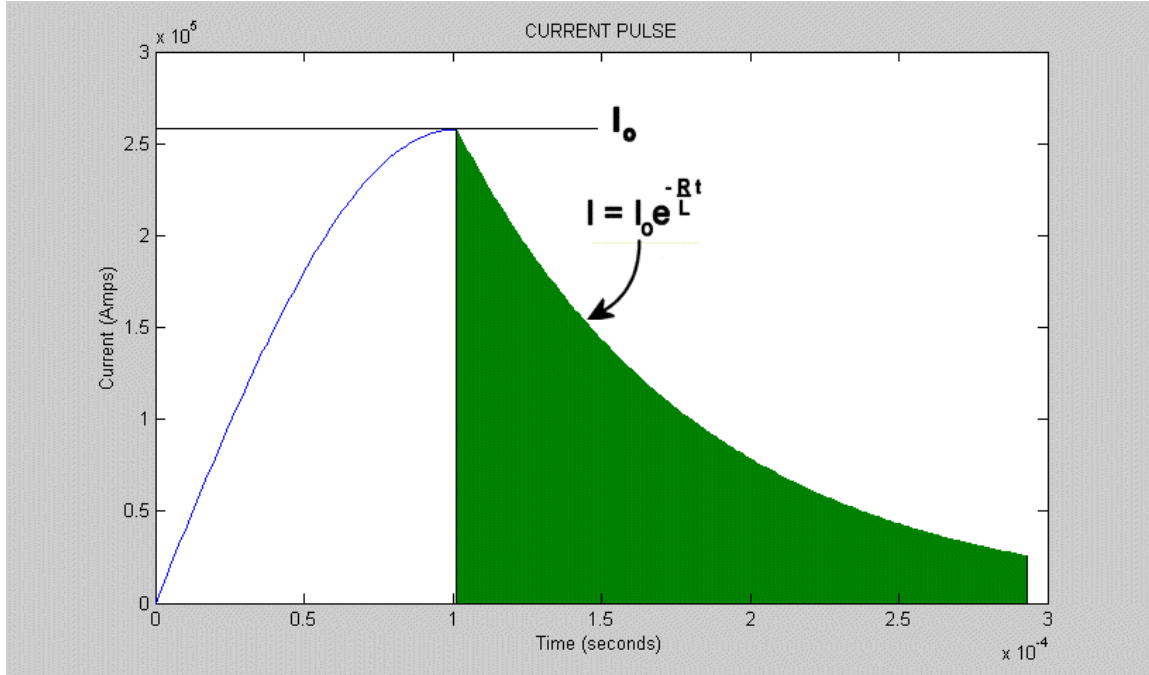


Figure 6. Waveform of a current pulse.  $L = 2.5 \mu H$ ,  $C = 1660 \mu F$ ,  $R = 9 m\Omega$ , voltage across capacitors,  $V_c$ , is 2.25 kV.

The inherent inductance of the power supply and rail gun together is  $2.5 \mu H$  which results in a short current pulse. The current is large for only a very short portion of the 4-inch rails. To stretch the current pulse additional inductance is added. By widening the current pulse, a large current passes through the projectile for a longer portion of the rails. The equation for calculating the magnitude of the current during the exponential decay (shaded portion) of the current pulse is given below:

$$I = I_0 e^{-Rt/L} \quad (2.1)$$

The variable  $I$  is the current value.  $I_0$  is the peak value of the current. The variable  $R$  is the resistance. The variable  $t$  is the time and  $L$  is the inductance.

A 30- $\mu H$  inductor was built according to the following equation:

$$n = \sqrt{\frac{L(9a+10b)}{a^2}} \quad (2.2)$$

The variable  $n$  is the number of turns for the entire coil. The inductance, measured in  $\mu H$ , is  $L$ . The variable  $a$  is the radius of the coil and  $b$  is the length in inches.

The 30- $\mu H$  inductor with a diameter of 1.5 feet and length of 10 inches was built. This inductor withstood currents at power supply capacitor voltages up to 5500 volts.

Figure 7 shows the current waveform when the capacitors have been charged to 1 kV. The 30- $\mu H$  coil is not yet placed in the circuit, so the circuit inductance is 2.5  $\mu H$ . The peak current is approximately 13 kA.

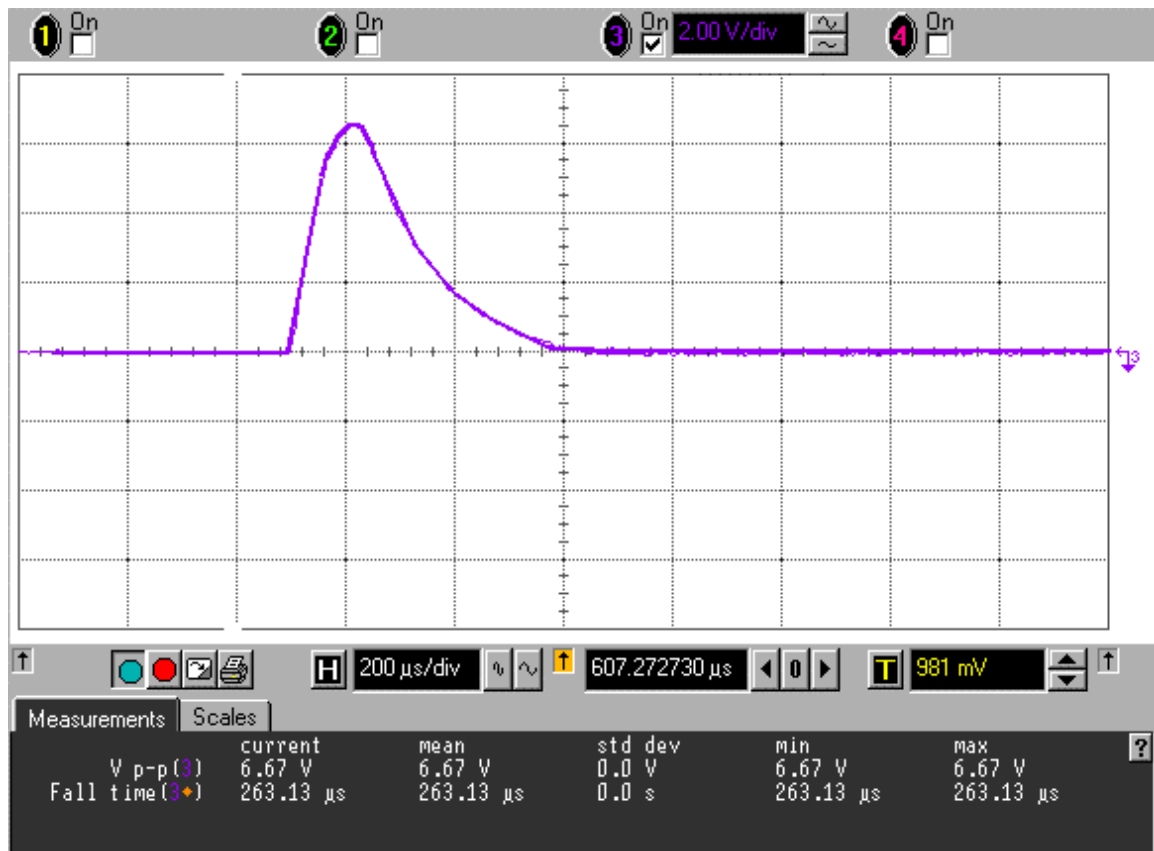


Figure 7. Current pulse without inductor. The ordinate scale is 2 V per major division. The abscissa scale is 200  $\mu$ s per major division.

Figure 8 shows the current waveform with the 30- $\mu$ H inductor inserted between the power supply and the positive rail gun pole. The current waveform now has a longer time constant, of approximately 2 ms. The peak current is reduced to approximately 8 kA

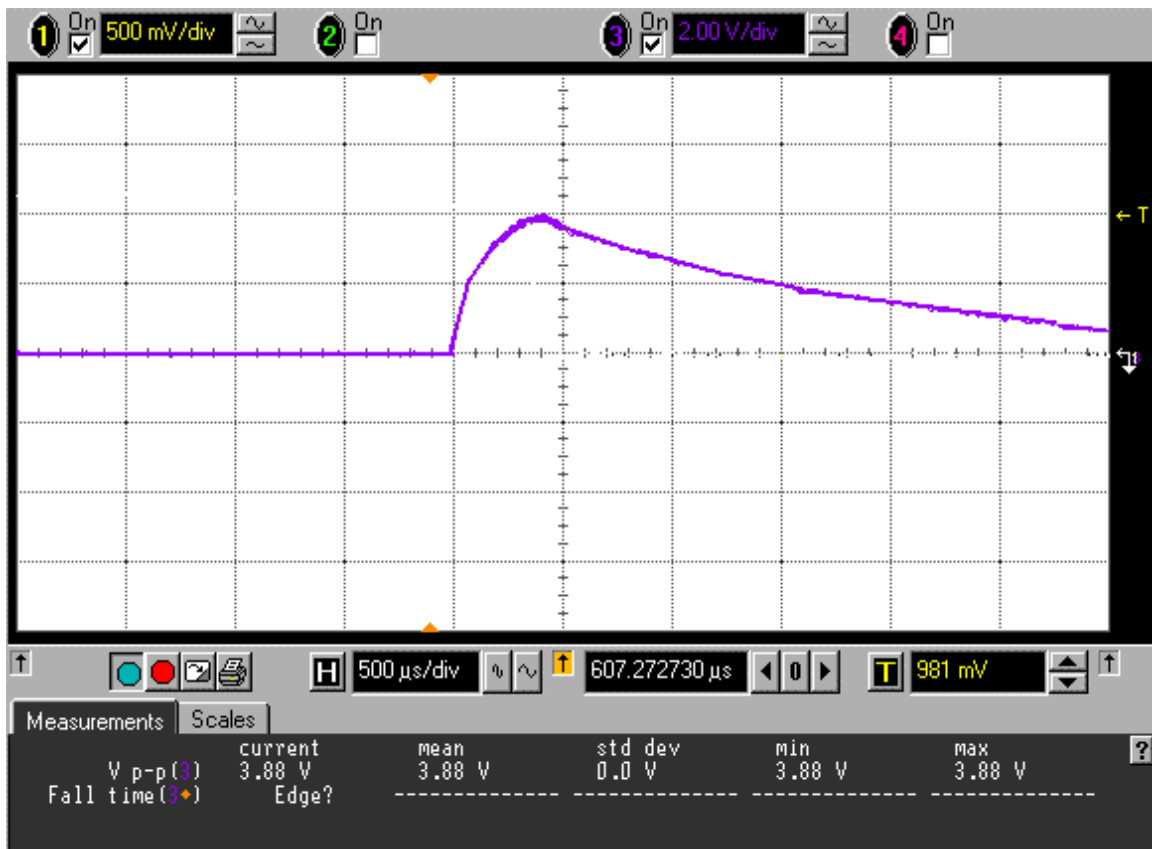


Figure 8. Current pulse with inductor. Vertical sensitivity is 2 V per division. Horizontal sensitivity is 500  $\mu$ s per division.

#### D. CURRENT DENSITY

It was imperative that tests were conducted at a consistent current density. To mimic the current densities expected for a Naval rail gun, currents of 10 kA were used. It was necessary to see what power supply voltage 10 kA of current corresponded to.

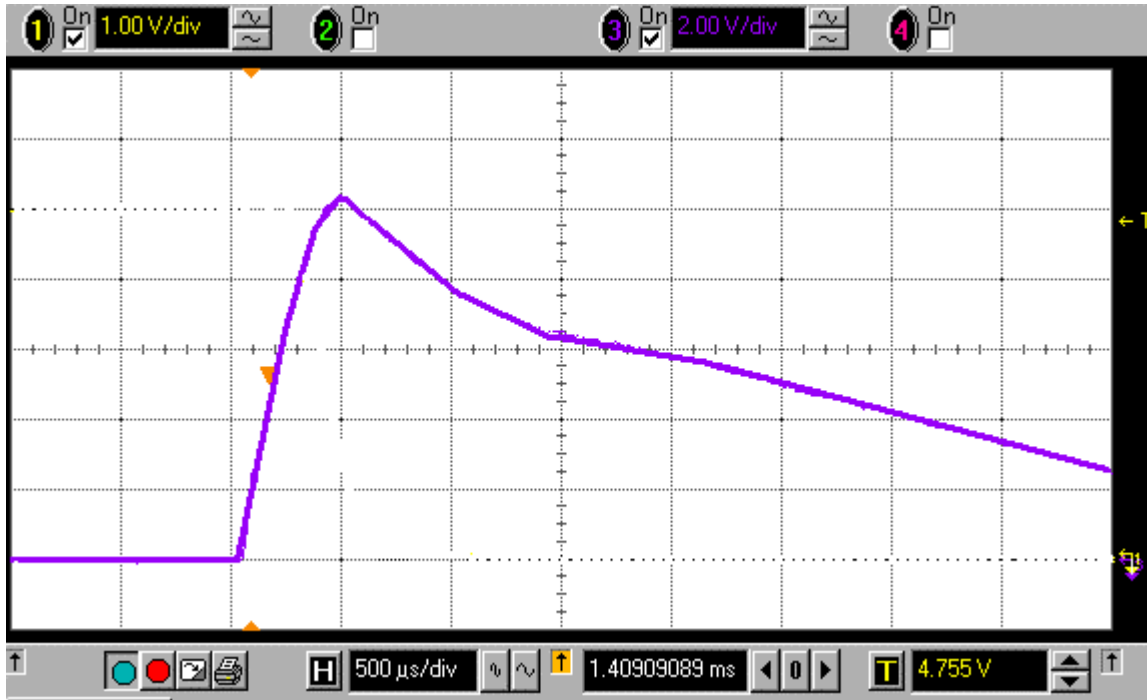


Figure 9. Current pulse. Ordinate scale is 2 V per division. Abscissa scale is 500  $\mu$ s per division.

In Figure 9, the current pulse is the solid line. A Pearson Transformer with a sensitivity of  $5 \frac{mV}{A}$  was used to generate the current waveform. For more details regarding to the Pearson Transformer please refer to Adamy's thesis [1].

The capacitors were charged to 2 kV and then discharged into the empty rail gun. The voltage peak to peak of the current waveform is 10.41 V. There is a 10:1 voltage divider connecting the power supply to the Pearson Transformer. Therefore, the current can be calculated using the following equation.

$$I_{peak} = \frac{V_{p-p} \times 10}{5 - mV/A} = 2000 \times V_{p-p} \quad (2.3)$$

The voltage peak to peak,  $V_{p-p}$ , is 10.41 V. Equation 23 gives a peak voltage of 20,800 A, or an average current of 10.4 kA over 3 ms. When the capacitors are charged to 2 kV, there is 3.3 kJ of energy in the system [6]. Later tests were conducted at 1 kV and approximately 5.2 kA of average current.

## E. PARTS

### 1. Accelerator

Adamy used an ME Schermer Captive Bolt Cattle Stunner as a projectile accelerator. The stunner consists of a 175-gram bolt that extends out of the housing a distance of 7.5 cm when fired. Three rubber rings stop the bolt's momentum. A small cartridge is used to accelerate the bolt.

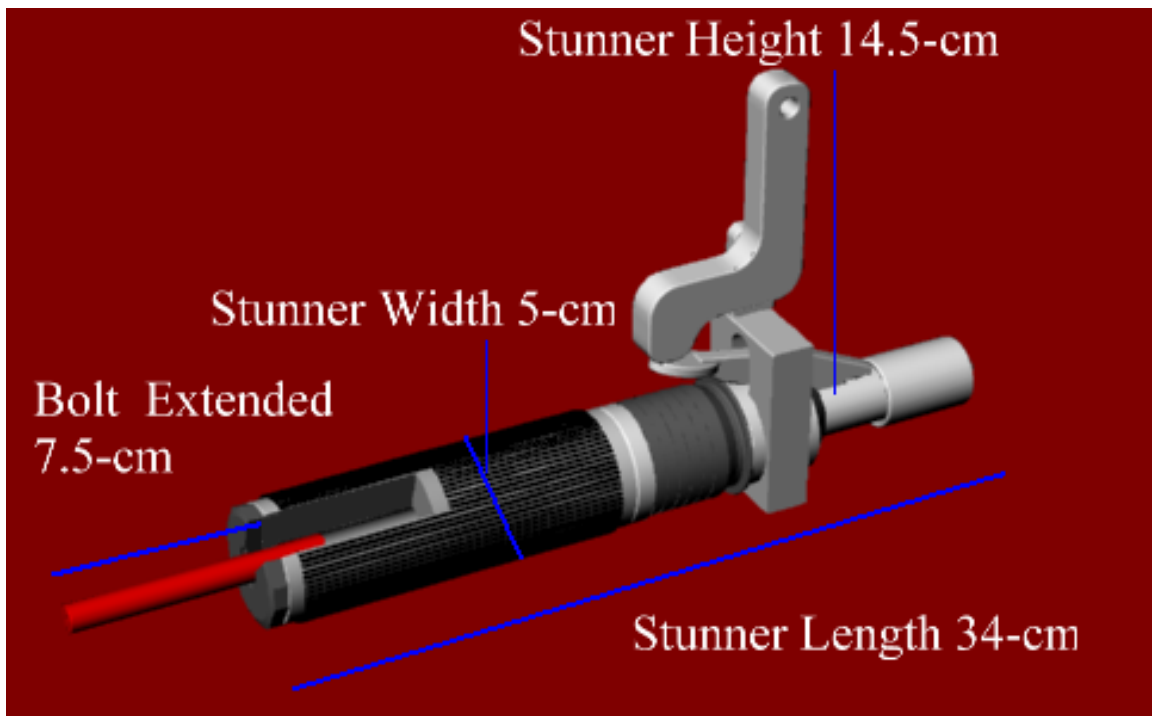


Figure 10. Drawing of the accelerator

Figure 10 shows the Schermer Captive Bolt stunner. The cartridge housing can hold one of four different cartridges. The three most powerful cartridges: yellow #13, red #17, and black #21 were used during testing.

**a. Determining the Velocity of the Captive Bolt**

It was necessary to know how fast the stunner's bolt traveled when fired with these three different cartridges. To make this measurement, two lasers were placed across from two separate photo detectors. The laser beams were spaced 5 cm apart.

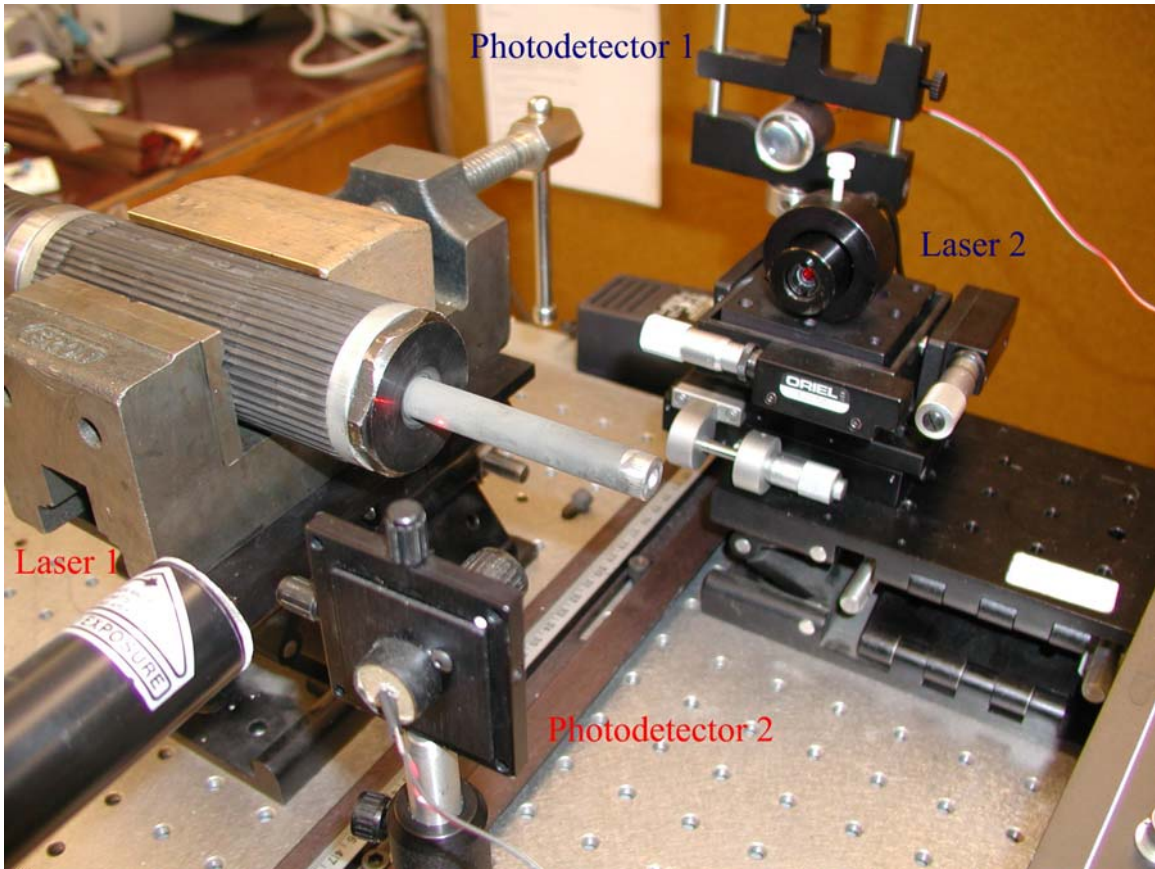


Figure 11. Picture of Laser Setup

Figure 11 shows how the two lasers and photo-detectors were positioned. Each photo detector was then wired to a LF-411 operational amplifier. The output of each LF-411 was displayed on an oscilloscope so that velocity measurements could be recorded.

The stunner was fired five times for each cartridge. The following table summarizes the results.

Table 2. Cartridge Velocities

<b>Cartridge</b>	<b>Time</b>	<b>Average Velocity</b>	<b>Average Deviation</b>
Yellow	1.25 ms	40.0 m/s	2 m/s
Red	1.15 ms	43.5 m/s	4 m/s
Black	1.00 ms	50.0 m/s	8 m/s

There were consistently problems with the black cartridge. The 8 m/s average deviation for the black cartridge resulted because it was difficult to secure the stunner properly with this high power cartridge. Eventually, the stunner was fired with a black cartridge that fractured the steel pusher housing and destroyed the pusher assembly.

Yellow and red cartridges were used for all later tests, so that parts could be used for longer periods of time without repairs. The figure below illustrates the data obtained from the oscilloscope for a yellow cartridge.

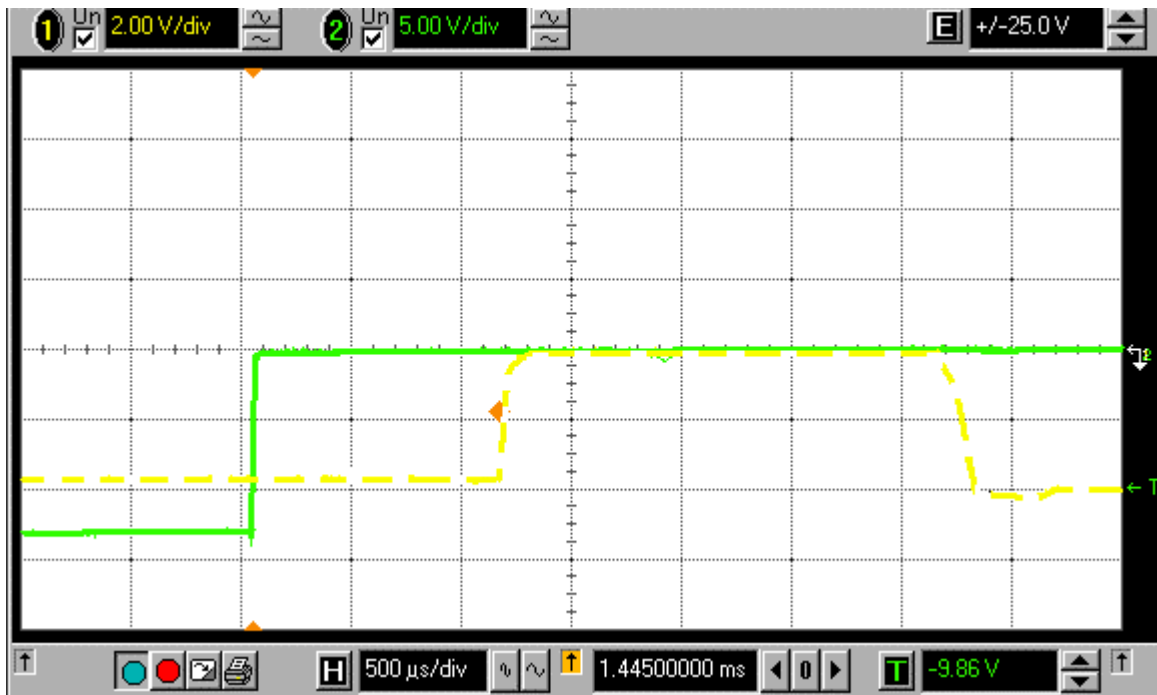


Figure 12. Waveform of bolt passing through lasers. Ordinate and abscissa scales are 2 V per division and 500  $\mu$ s respectively.

The steep rise of the solid curve is when the bolt breaks the first laser beam. The broken curve rises sharply when the bolt interrupts the second laser beam. It took approximately 1.25 ms for the bolt to pass through the first laser beam and interrupt the second. The distance the bolt traveled between the two beams is 5 cm. Therefore, the velocity is calculated to be 40 m/s.

## 2. Pusher Housing

The pusher housing holds the pusher assembly and has two ports where two fiber optic cables are attached. The chamber's length was 4.5 inches. The ports were also modified to handle thicker fiber optic cable. The fiber-

optic cables are inserted into the two ports so that the capacitors can be triggered to discharge when the light path between the two ports is interrupted. For a more detailed explanation of this process please refer to Mark Adamy's thesis [1]. Two 0.125-inch neoprene disks were punched and placed on the end of the housing so that the pusher housing would not damage the rail gun when the stunner is fired.

### 3. Pusher Assembly

The actual pusher consists of a base piece and a phenolic rod. The base piece is a disk composed of hardened aluminum, and a steel cylinder support. Figure 13 shows the base and the steel support within the pusher housing.

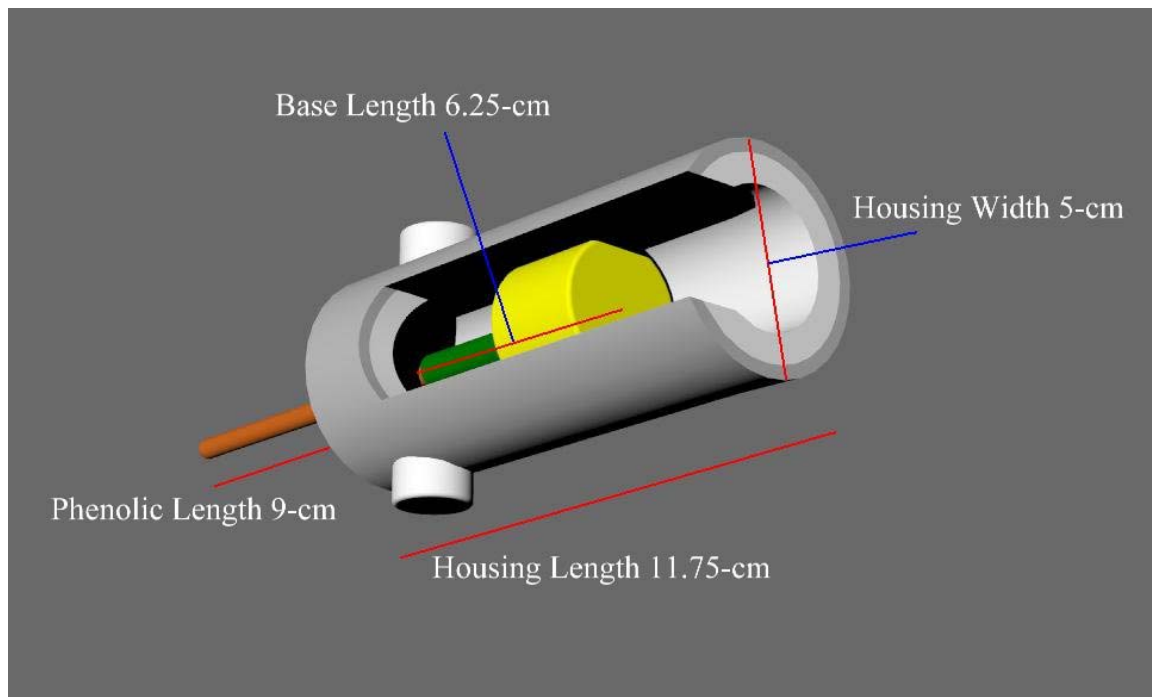


Figure 13. Pusher housing and assembly dimensions

The base's length was reduced by 1 inch from the length used by Mark Adamy, so that the overall weight of the pusher was 175 g in order to obtain good momentum transfer from the bolt to the pusher. An aluminum disk is placed at the end of the aluminum base so that the base is not damaged when the bolt strikes it. The phenolic rod length is chosen so that it would only push the projectile for 0.25 in.

#### **F. TRIGGER BOX AND DELAY GENERATOR**

The "Delay Generator" is a Four Channel Digital Delay/Pulse Generator, model DG 535, built by Stanford Research Systems Incorporated. Once the base of the pusher assembly breaks the light beam from the two fiber optic cables running to the pusher housing, a signal is sent to the delay generator. The delay generator then switches the TVS-40 high voltage switch, which in turn discharges the capacitor bank.

#### **G. CONTACT BOX**

Determining how well the projectile maintains contact with the rails as it is accelerated is a vital piece of information when rail and barrel wear are being analyzed. If the projectile loses electrical contact, then arcing will result which is very harmful to both rails and projectiles [3]. A "contact box" was made to measure how well the projectile maintains electrical contact as it is accelerated through the rails without any current being present. First, contact was measured when the stunner

accelerated the projectile without any current. Yellow cartridges were used during these tests. A sketch of the circuit used to measure the voltage across the rails is given in the figure below. Results will be shown in Chapter 3.

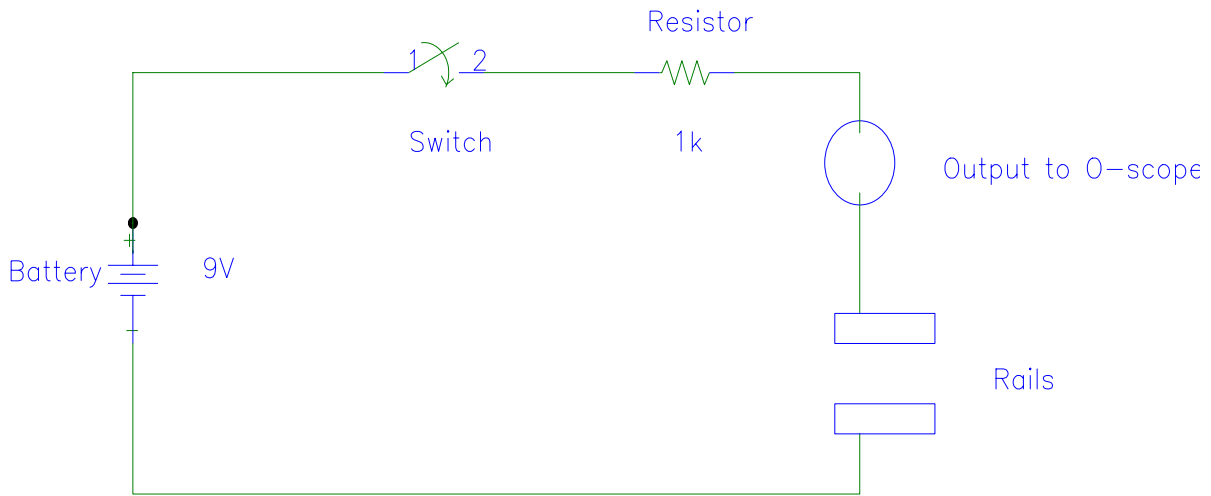


Figure 14. Circuit of contact box

## H. INTERIOR AND EXTERIOR DIAGNOSTICS

Two of the main goals of this thesis research were to develop a means of measuring the voltage drop across the rails during the high current flow, and to measure the projectile's velocity as it exits the rail gun.

### 1. Variable Graphite Resistor

Obtaining the voltage drop across the rails was accomplished by making a variable compressible resistor. The resistor uses graphite squares stacked together and compressed in a vice. When the vice tightens, the

resistance decreases. The resistor was lined with two sheets of phenolic so that the graphite would not come into contact with the steel housing. A thin square brass piece was inserted between two of the graphite plates so that the resistor would act as a 10:1 voltage divider. The resistor was then connected to an analog oscilloscope. Figure 15 shows how the resistor was positioned across the two rails. See Figure 5 for a circuit schematic.

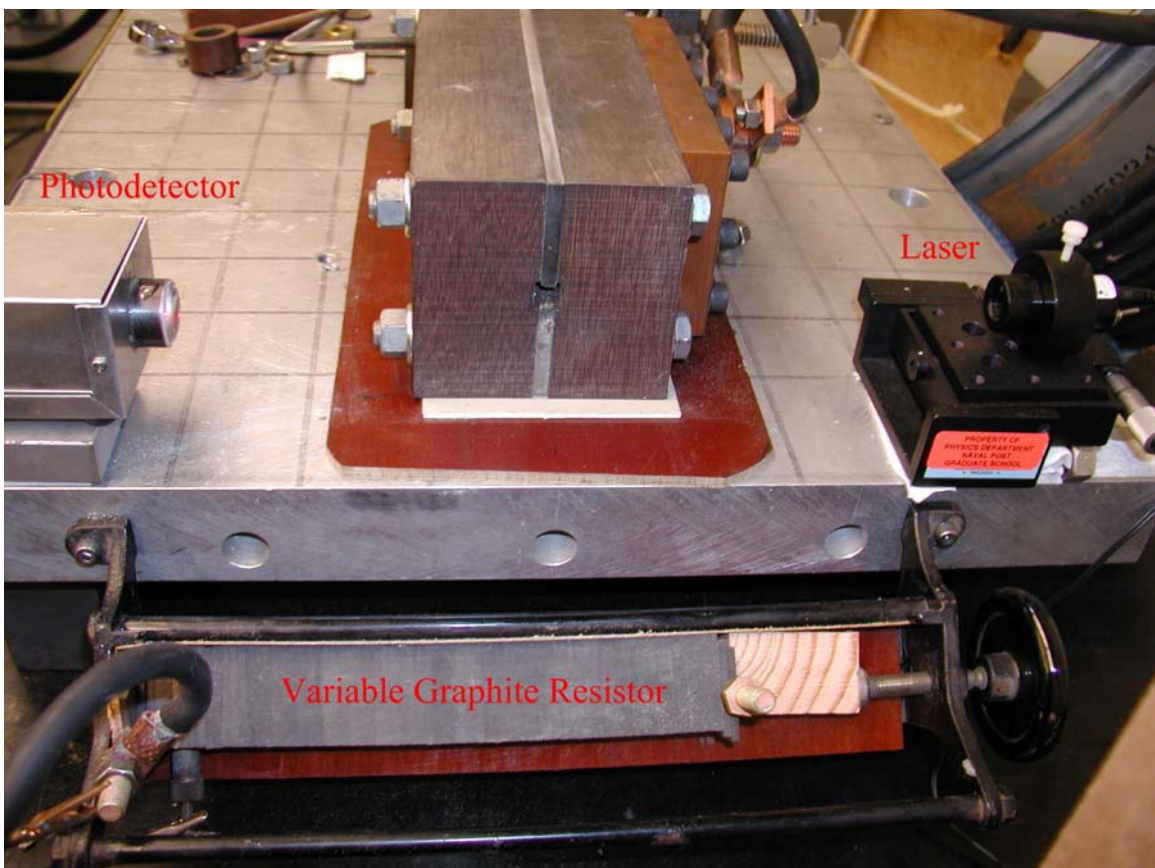


Figure 15. Laser and Variable Resistor Position

The graphite resistor had to handle high current. The capacitor bank was charged to 2.5 kV, and then discharged

directly into the resistor. The resistor was able to handle the resultant current of 13 kA.

The resistor was eventually mounted in front of the rail gun so, that the leads connecting the resistor to the pole pieces could be as short as possible in order to prevent inductive pickup. In the end, the leads from the resistor to the pole pieces were 13 inches each.

An oscilloscope with a differential amplifier was used in order to measure the difference in voltage across the rails, and to reduce common mode pickup. An Analog Tektronix Oscilloscope, model 7603, was used to obtain waveforms of the voltage drop across the two rails. A Digital Tektronix camera, model C1002, relayed the waveform to a computer so that data could be stored and analyzed at a later date.

## **2. Laser for Projectile Velocity Measurement**

The second major goal at the start of this thesis was to determine the velocity of the projectile as it exited the barrel. An attempt to use a Chronograph from Shooting Chrony Incorporated failed.

Eventually, a simple design utilizing a diode laser and a photo-detector was devised. A laser and a photo detector were placed across from one another and 1 cm in front of the bore of the rail gun. Figure 15 shows how the laser and photo-detector were positioned in front of the rail gun.

A circuit like the one used to measure the stunner's bolt velocity was used to measure the projectile's

velocity. The pusher assembly triggers the capacitors to discharge when the phenolic rod is flush against the projectile. At this point the oscilloscope will begin displaying data. After this point the projectile is traveling through the rails. When the projectile exits the bore, the laser beam will be broken.

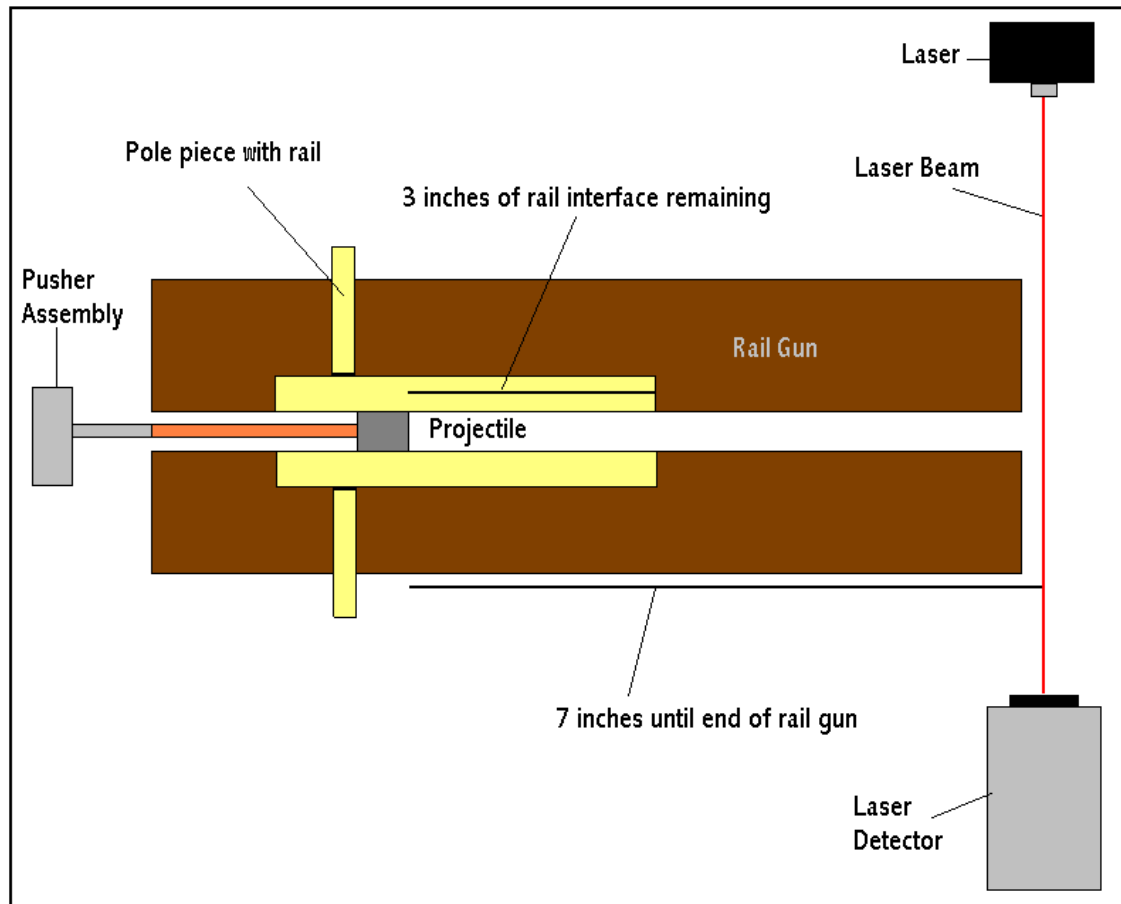


Figure 16. Dimensions of laser setup

Figure 16 shows the projectile placement with 3 in of rail remaining.

## I. THERMAL LOADING OF RAILS

The projectile in the 4-inch rail gun can be fired in a manner that approximates thermal loading of the rails in a much larger Naval Rail Gun.

The power,  $P$ , dissipated at the interface between the rails and projectile is:

$$P = RI^2 \quad (2.4)$$

and the work is given by:

$$W = Pt = RI^2 t \quad (2.5)$$

where,  $I$  is the current,  $R$  is the resistance, and  $t$  is the time the projectile is in contact with a given point on the rails. The time is given as  $\frac{Z}{v}$ .  $Z$  is the length of the projectile and  $v$  is the projectile's velocity. The resistance can be expressed as:

$$R = \frac{\rho x}{A} \quad (2.6)$$

Where the variable  $\rho$  is the resistivity of the material used to construct the rails, and  $x$  is the interface depth.  $A$  is the area of the projectile's surface that is in contact with the rails.

Substituting for the resistance and current in Equation 2.4 yields:

$$W = \frac{\rho x I^2 Z}{A v} = \frac{\rho Z A J^2 x}{v} \quad (2.7)$$

Equation 2.7 can then be manipulated to yield:

$$\frac{W}{Ax} = \frac{\rho Z J^2}{v} \quad (2.8)$$

Where the current density,  $J$ , is  $\frac{I}{A}$ . Equation 2.8 is the work per unit area multiplied by the interface depth, a value that correlates to the energy available for transfer to the rails during the projectile passage. Estimates of  $\frac{W}{Ax}$  are compared in Table 3 for the Naval Rail Gun and the NPS 4-inch Rail Gun.

The values for  $Z$ ,  $J$ , and  $v$  are given in Table 3.

Table 3. Parameters for calculating  $\frac{W}{Ax}$

Variable	Navy Rail Gun	NPS Rail Gun
$Z$ [m]	0.5	0.0063
$J$ $\left[ \frac{A}{m^2} \right]$	$2.5 \times 10^8$	$2.5 \times 10^8$
$v$ [m/s]	2000	50
$\frac{W}{Ax} \left[ \frac{A^2 s}{m^4} \right]$	$1.56 \times 10^{13} \times \rho$	$7.88 \times 10^{12} \times \rho$

The current density,  $J$ , was set to  $2.5 \times 10^8 \left[ \frac{A}{m^2} \right]$  which is derived in Gillich's thesis [6]. The resistivity,  $\rho$ , will

be similar for the NPS and Navy rail gun. Thermal loading of the rails for the Naval rail gun is calculated to be  $1.56 \times 10^{13} \times \rho \left[ \frac{A^2 s}{m^4} \right]$ . The NPS thermal loading is calculated to be  $7.88 \times 10^{12} \times \rho \left[ \frac{A^2 s}{m^4} \right]$ . The values for thermal loading,  $\frac{W}{Ax}$ , are thus similar in the NPS test rail gun and the Naval rail gun. The parameters in Equation 2.8 can be adjusted in the future so that the comparison is even closer.

### **III. TEST RESULTS**

#### **A. STATIC TESTS WITH CONTACT BOX**

The contact box that was built measures the voltage difference across the rails without any current present. The stunner was the sole means of accelerating the projectile during these tests. The purpose of this testing was to see how well the projectile maintained contact on dry rails, and if coating the rails with a substance helped the projectile maintain contact. A projectile was placed between two dry grooved rails. The stunner was fired into the pusher assembly with a yellow cartridge. The voltage across the rails as the projectile moves down the interface is shown in Figure 17.

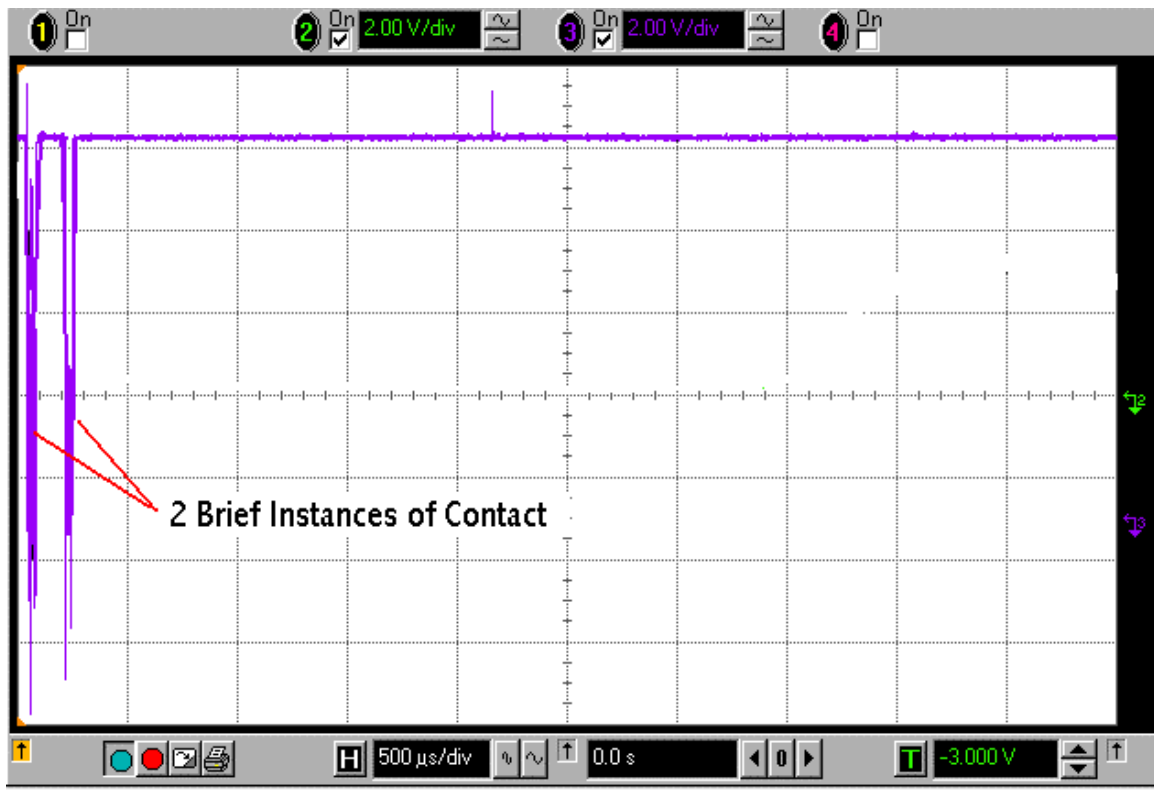


Figure 17. Observed voltage for firing with bare rails. The ordinate and abscissa scales are 2 v per division and 500  $\mu$ s per division respectively.

As soon as the projectile breaks contact, the voltage settles to positive 6 volts. When the projectile is in contact with the rails the voltage briefly reads -6 v, then 0 v. Figure 17 shows that the projectile is hardly ever in contact with the rails.

The rails were then removed, cleaned, and coated with a thin layer of silver paste. A projectile was placed in the same position and the stunner was fired with a yellow cartridge. The following figure shows the voltage across the silver coated rails.

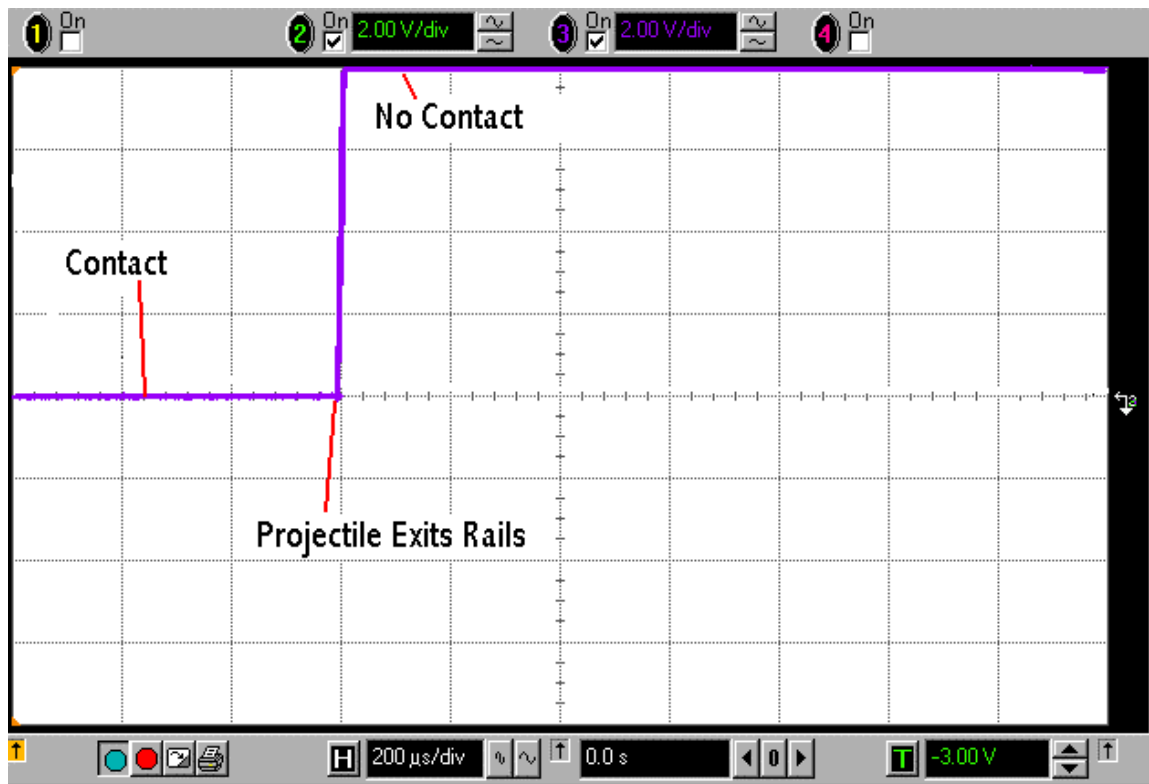


Figure 18. Waveform of contact with silver paste.

The vertical scale is 2 V per division. The horizontal scale is 200  $\mu$ s per division.

Here, the projectile is making electrical contact when the voltage is at 0 volts. The steep rise to just over 8 volts occurs when the projectile exits the rails. The projectile travels the 3 inches of rail in 600  $\mu$ s. This gives a velocity of 125.3 m/s. This value does not match other velocity measurements. One possibility for this difference is that the beginning of this waveform was not recorded. The above figure still illustrates a key point, that the projectile maintains better electrical contact when rails coated with silver paste are used.

## B. PROJECTILE VELOCITY RESULTS

The laser was positioned as shown in Figure 16. Results are given in the figure below. Tests to record the projectile's velocity were conducted by charging the capacitors to 1 kV. The peak current running through the rails was 8 kA. The average current running through the rails was approximately 5 kA. The description of the projectiles used can be found in Chapter 2, Section A.

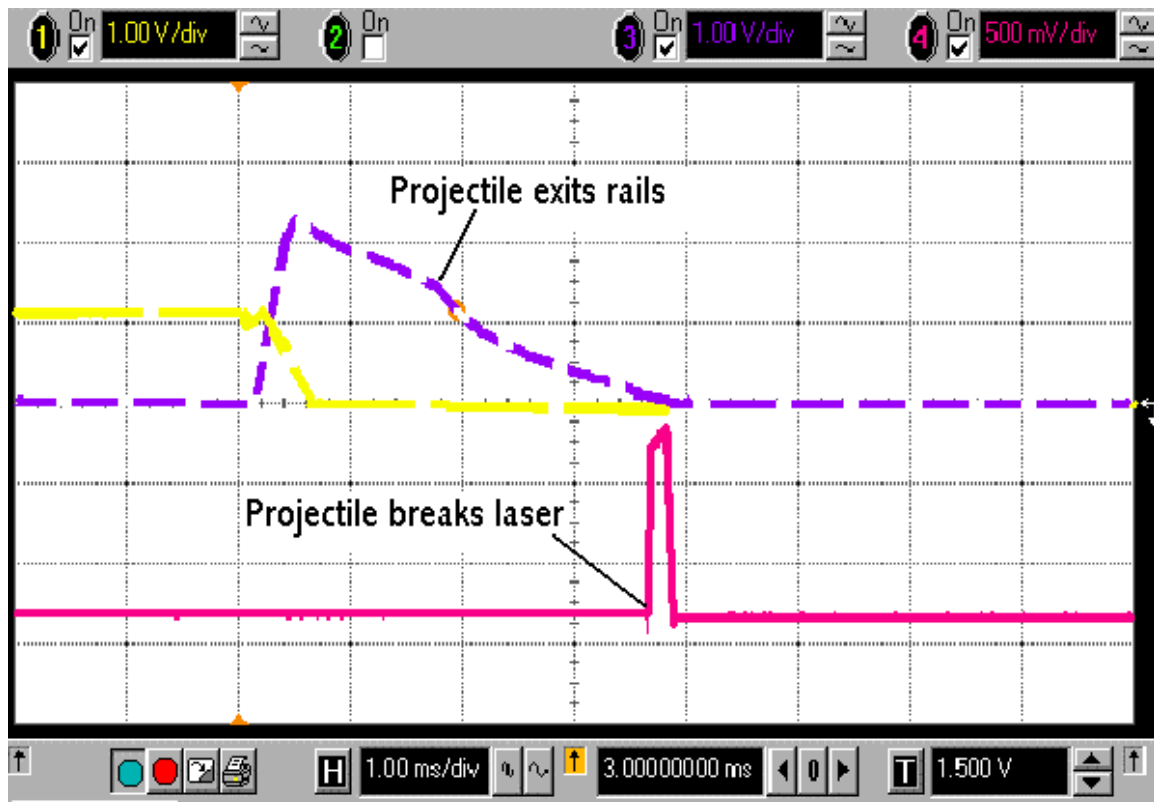


Figure 19. Waveform of Projectile Position. The ordinate scale is 1 V per division. The abscissa scale is 1.00 ms per major division.

In Figure 19, the solid line shows when the projectile passes through the laser. The dashed line is a waveform of the current pulse. The broken line is the voltage across the capacitors.

The projectile travels 7 in before passing through the laser. From the solid waveform, it took 3.5 ms for the projectile to travel this distance. The projectile's average velocity along the barrel is 50.8 m/s.

The dashed line shows the current as a function of time. The slope of the curve changes when the projectile exits the rails. The sudden increase in the solid curve indicates when the projectile exits the rail gun. For this shot, it took approximately 1.5 ms for the projectile to exit the rails. The projectile traveled 3 inches in 1.5 ms, which translates to a velocity of 50.8 m/s.

#### C. RESULTS WITH THE VARIABLE RESISTOR

##### 1. STATIC TESTS WITH VARIABLE RESISTOR

Static tests were performed with the compressible resistor mounted in front of the rail gun. Leads from the power supply were connected to the rail gun. A projectile was not placed between the rails in order to see what the waveform would look like when the projectile is not in contact with the rails. The capacitors were charged to 1 kV and then discharged into the empty rail gun. The following figure shows the waveform when there was not a projectile placed inside the rail gun. The following four figures have a vertical sensitivity of 2 V per division and

a time-scale of 500  $\mu$ s per division. The voltage drop, shown in Figure 20, is similar to the expected current pulse.

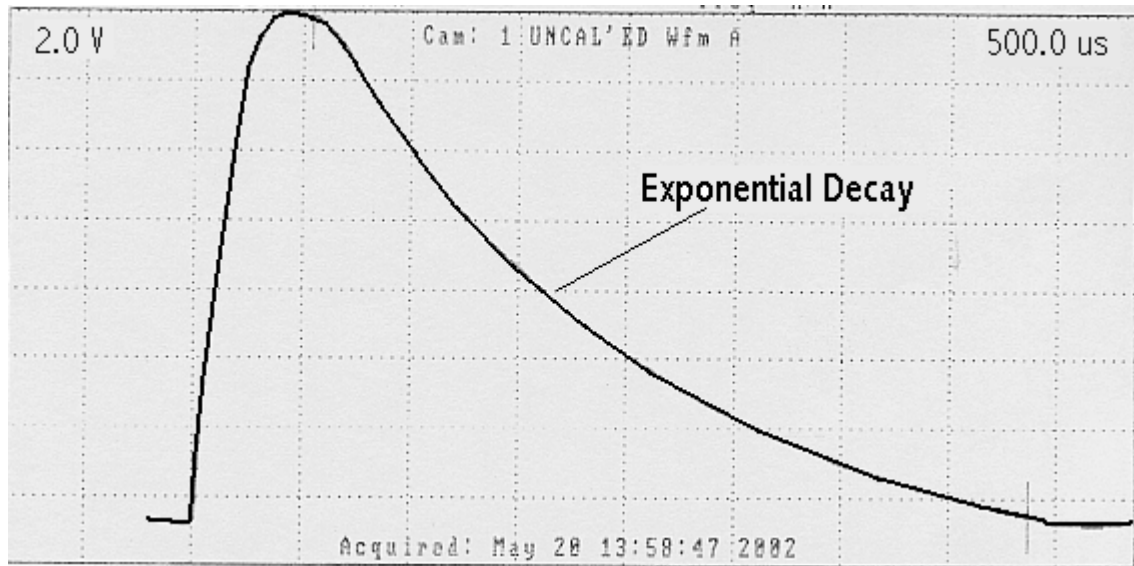


Figure 20. Voltage across empty rails. The ordinate and abscissa scales are 2 V per division and 500  $\mu$ s per division respectively.

The next step is to place a projectile between the rails and discharge the capacitors at 1 kV in order to see the waveform when there is contact between the projectile and the rails. For this test the rails are tightened down so that the projectile would not move during a 1 kV shot. The exact position of the projectile is marked on the rails in order to see if the projectile moves once the capacitors are discharged. After the capacitors were discharged, the rails are inspected and it is clear that the projectile is still in the same position. Figure 21 shows the voltage when the projectile is in contact with the rails.

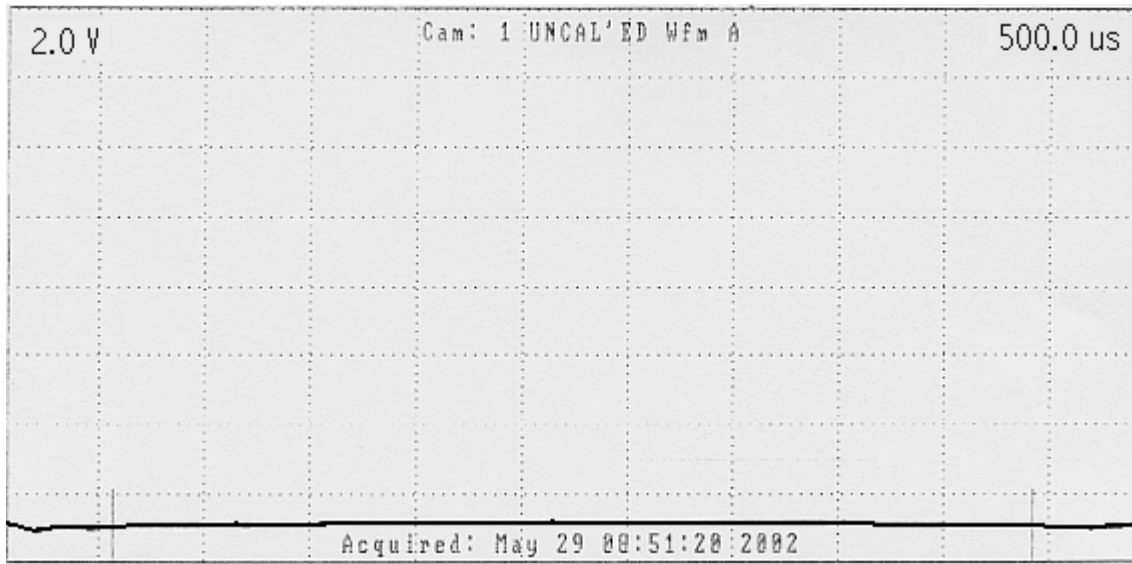


Figure 21. Voltage across rails for a static projectile in good electrical contact. The ordinate and abscissa scales are 2 V per division and 500  $\mu$ s per division respectively.

The next step is to inject a projectile through the rails and see how well it maintains contact when the power supply is discharged.

## 2. Dynamic Tests With Variable Resistor

During dynamic testing a 0.25-inch wide projectile was placed 1 inch from the rails starting point. The rails were tightened so that it was difficult to move the projectile. A string was attached to the stunner and ran through a pulley so that no one was close to the power supply when it discharged. The stunner accelerated the projectile once triggered. The light beam through the pusher housing was then interrupted which triggered the capacitors to discharge.

The first test was done with dry grooved rails. Refer to Figure 16 for projectile placement. The capacitors were

discharged at 1 kV, which correlates to 5 kA of average current. The peak current was approximately 8 kA.

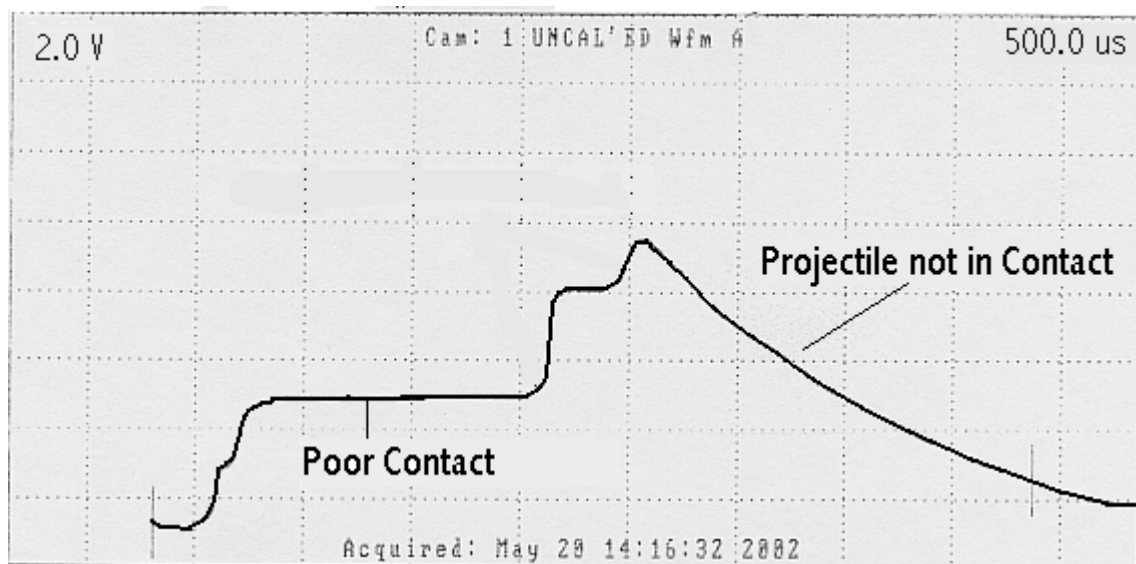


Figure 22. Voltage drop when projectile traveled through dry grooved rails. The ordinate and abscissa scales are 2 V per division and 500  $\mu$ s per division respectively.

Figure 22 shows that the projectile is in contact with the rails at the very beginning of the waveform. As the projectile is accelerated, electrical contact is less good and the indicated voltage across the rails rises to a higher value. Once the projectile exits the rails and the resulting electrical discharge has ceased, the current decrease is mostly governed by circuit inductance and the 0.03-ohm resistor in Figure 5.

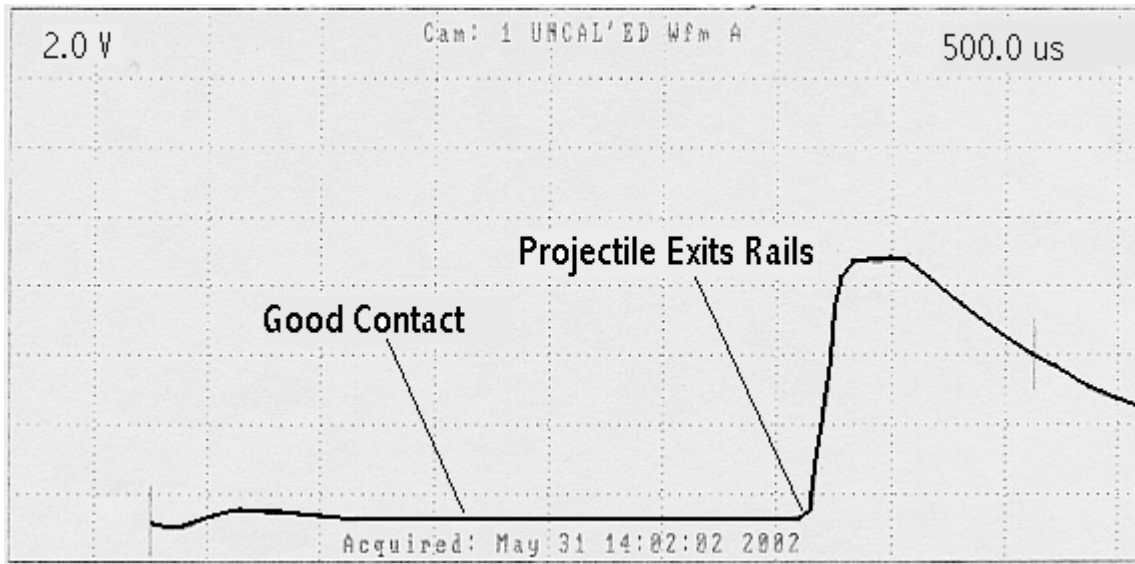


Figure 23. Voltage drop when projectile traveled through rails coated with silver paste. The ordinate and abscissa scales are 2 V per division and 500  $\mu$ s per division respectively.

Now, the rails will be coated with silver paste to see if this helps the projectile maintain better electrical contact. Figure 23 shows that the addition of silver paste allowed for good electrical contact to be established while the projectile moved along the full length of the rails.

#### D. RAIL EROSION

It has been shown that better electrical contact was obtained by coating the grooved rails with silver paste. The next goal was to analyze how well silver paste limited rail erosion. First, dry rails were used in order to record the damage. The stunner was loaded with a yellow cartridge and fired into the pusher assembly. The power supply was triggered once the pusher assembly broke the light beam inside the pusher housing. The projectile was

placed 3 inches from the exit end of the dry rails. The force from the stunner along with the Lorentz Force accelerated the projectile through the bore of the rail gun. Pictures of the rails were then taken in order to show the wear on the rails.



Figure 24. Wear on dry grooved rails

Figure 24 shows the damage that resulted when the capacitors were discharged at 1 kV. There was 8 kA of peak current and 5 kA of average current running through the rails.

The rails were then removed and replaced by clean rails, that were coated with a thin layer of silver paste, as illustrated in the figure below, in order to establish electrical contact and inhibit damage to the rails and the projectile.



Figure 25.      Rails coated with silver paste before firing

The rail gun was then loaded with a projectile placed in the same position, 3 inches from the exit end of the rails. The stunner was again loaded with a yellow cartridge and fired. After the stunner was fired and the power supply was triggered, the rails were removed and the

excess silver paste was wiped off. No damage was found visually for this shot on either rails or projectile.



Figure 26. Projectile and rails coated with silver paste after shot

These tests accelerated the projectile to an average velocity of 50 m/s. The average current that was given to the rail gun was 5 kA. The silver paste helped the projectile maintain electrical contact with the rails, which in turn significantly limited the erosion that the rails and projectile experienced.

#### IV. CONCLUSION

The four-inch-rail gun used for testing purposes at NPS has been improved. Modifications to the Adamy design allowed for ways to determine interior and exterior projectile diagnostics. The power supply was also reconfigured in order to measure the voltage drop across the rails when the sliding contact is traveling through the rail gun.

A variable graphite resistor allows one to measure how well the projectile is maintaining electrical contact by analyzing the voltage drop across the rails. A diode laser was also integrated into the existing rail gun configuration so that the projectile's velocity could be accurately measured.

The rail erosion problem has also been analyzed with some success. The results in Chapter 3 show that silver paste significantly reduces erosion on both the rails and projectile. The presence of silver paste increases the electrical contact between the rails and projectile, therefore decreasing the amount of erosion that occurs upon firing. More tests need to be conducted in order to determine other possibilities for the rail-projectile interface.

THIS PAGE INTENTIONALLY LEFT BLANK

## V. FUTURE WORK

More shots and testing with the NPS 4-inch Rail Gun must be conducted. Time was a major factor in determining how many tests were completed successfully for this thesis. Materials other than silver paste also must be tested. Silver paste does a good job of maintaining electrical contact between the rails and the projectile, but other materials might be even better. For convenience of display, the voltage across the rails should be put into a fully isolated differential amplifier, and the output from the amplifier fed into the oscilloscope monitoring capacitor voltage, current, voltage across the rails, and projectile exit. The tests should also be run at currents up to 20 kA.

THIS PAGE INTENTIONALLY LEFT BLANK

## LIST OF REFERENCES

1. Adamy, M.T., *An Investigation of Sliding Electrical Contact in Rail Guns and the Development of Grooved-Rail Liquid-Metal Interfaces*.
2. Beach, F.C., *Design and Construction of a One Meter Electromagnetic Railgun*, Master's Thesis, Naval Postgraduate School, Monterey, California, June 1996.
3. Colombo, G.R., Otooni, M., Evangelisti, M.P., Colon, N., and Chu, E., *Applications of Coatings for Electromagnetic Gun Technology*, IEEE Transactions on Magnetics, Vol. 31, No.1, 1995.
4. Electro-Magnetic Launch Workshop at the Institute for Advanced Technology, Austin, Texas. 7-9 November, 2001.
5. Feliciano, A.S., *The Design and Optimization of a Power Supply for a One-Meter Electromagnetic Railgun*, Master's Thesis, Naval Postgraduate School, Monterey, California, December 2001.
6. Gillich, D.J., *Design, Construction, and Operation of an Electromagnetic Railgun Test Bench*, Master's Thesis, Naval Postgraduate School, Monterey, California, June 2000.
7. Gurhan, Ozkan, *A methodology to Measure Metal Erosion on Recovered Armatures*, Master's Thesis, Naval Postgraduate School, Monterey, California, December 2001.
8. Lockwood, M.R., *Design and Construction of an Expandable Series Augmented Electromagnetic Railgun*, Master's Thesis, Naval Postgraduate School, Monterey, California, June 1999.
9. Luke, I.T. and Stumborg, M.F., *The Operational Value of Long Range Land Attack EM Guns to Future Naval Forces*, IEEE Transactions on Magnetics, Vol. 37, No.1, 2001.
10. Marshall, R.A., *Railgunnery: Where Have We Been? Where Are We Going?*, IEEE Transactions on Magnetics, Vol. 37, No.1, 2001.

11. McNab, I.R., Fish, S., and Stefani, F., *Parameters for an Electromagnetic Naval Railgun*, IEEE Transactions on Magnetics, Vol. 37, No. 1, 2001.
12. Nearing, J.C. and Huerta, M.A., *Skin and Heating Effects of Railgun Current*, IEEE Transactions on Magnetics, Vol. 25, No. 1, 1989.
13. Stefani, F., Levinson, S., Satapathy, S., and Parker, J., *Electrodynamic Transition in Solid Armature Railguns*, IEEE Transactions on Magnetics, Vol. 37, No. 1, 2001.

## **INITIAL DISTRIBUTION LIST**

1. Defense Technical Information Center  
Ft. Belvoir, VA
2. Dudley Knox Library  
Naval Postgraduate School  
Monterey, CA
3. Professor William B. Maier II, Code PH/Mw  
Department of Physics  
Naval Postgraduate School  
Monterey, CA
4. Professor Richard Harkins, Code PH  
Department of Physics  
Naval Postgraduate School  
Monterey, CA
5. Engineering and Curriculum Office, Code 34  
Naval Postgraduate School  
Monterey, CA
6. ENS William E. Culpeper  
4409 Glen Oaks Dr.  
Matthews, NC